Throughput and Delay Tradeoff Over 3D UAV Communication Network

Jue Gong, Cheng Zhan, Renjie Huang, Changyuan Xu
School of Computer and Information Science, Southwest University, Chongqing, China
Email: {gj1340172827, xcy202009}@email.swu.edu.cn, {zhanc, huangrj}@swu.edu.cn.

GLOBECOM 2022 - 2022 IEEE Global Communications Conference | 978-1-6654-3540-6/22/$31.00 ©2022 IEEE | DOI: 10.1109/GLOBECOM48099.2022.10000607

***Abstract*—Due to its high mobility, flexible deployment, and low cost, unmanned aerial vehicles (UAVs) have attracted wide attention in wireless communication in recent years. However, the delay requirements (e.g., video streaming, online game, etc.) may limit the UAV's mobility. In this paper, we consider a three-dimensional (3D) UAV communication network, where a UAV is employed to fly flexibly in 3D space to serve ground users with delay requirements. To characterize the fundamental tradeoff between throughput and delay, we introduce the minimum required rate for users and aim to maximize the minimum weighted sum of throughput and required rate for each user, via joint optimization of the 3D UAV trajectory as well as communication time and rate allocation. The formulated problem is a non-convex optimization problem, which is generally intractable. By decomposing the formulated problem into two subproblems, we propose an iterative algorithm by block coordinate descent and difference of two convex (D.C.) optimization as well as successive convex approximation (SCA) techniques. Finally, extensive simulation results show that our proposed solution outperforms baseline schemes and unveils the interesting insights and tradeoff between throughput and delay over 3D UAV communication networks.**

***Index Terms*—unmanned aerial vehicle (UAV), 3D UAV trajectory, throughput and delay tradeoff, resource allocation.**

I. Introduction

Thanks to the flexible mobility, low cost, as well as on-demand deployment, unmanned aerial vehicles (UAVs) are expected to have a lot of applications in beyond-fifth-generation (B5G) and sixth-generation (6G) wireless networks for aerial wireless platforms [1]–[3]. In particular, UAVs can be employed as aerial base stations (ABSs) for a backup when ground base stations (GBSs) are paralyzed by natural disasters, or complementing GBSs as communication assistance platforms for cellular network offloading [4]. Unlike the conventional wireless communication systems, because of their operability and flexibility, UAVs have a greater probability of establishing line-of-sight (LoS) links, which can help enhancing the performance of the present terrestrial communication system.

On the other hand, video and other media services are more and more popular, e.g., virtual reality, online game, etc, which puts great pressure on the serving capacity of existing wireless networks, leading to low Quality of Service (QoS) of users [5]. Thus, B5G and 6G networks are expected to provide different QoS guarantees for media applications over a wide range of networks. For example, when a user downloads a file with a latency requirement, other people may be playing a high-definition (HD) movie at the same moment, which also requires a minimum rate for moving playing. Therefore, we should try to optimize these different types of services for maximizing system throughput, while satisfying the heterogeneous delay requirements of different applications. Intuitively, for the UAV enabled applications, the UAV may move close to and serve one particular user with better channel quality to enhance throughput, while other users far away from the UAV may violate the delay requirement since their channel quality may get poorer. Therefore, there exists a fundamental tradeoff between throughput and delay for users, where the UAV's mobility may be limited by the delay requirement. The work in [6] studied the tradeoff between throughput and access delay in UAV communication with cyclical multiple access along a straight line UAV trajectory. The work in [7] maximized the minimum average throughput in UAV-enabled communication systems with delay consideration, via optimizing UAV trajectory as well as power and bandwidth allocation. In [8], the author divided the delay requirements into two categories, namely delay limited transmission and delay resistant transmission, based on which the throughput was maximized. However, the above work only assumed a straight-line scene or horizontal flight, while ignoring the fact that the UAV can move freely in three-dimensional (3D) space.

The air-to-ground (A2G) channels are more challenging to model compared with that of ground channels, since the A2G channels consist of more model parameters due to the 3D position of the UAV. Blocking (like buildings and trees), the main difficulty to tackle in A2G channels, can clog transmission signals or reduce their power. In general, LoS and non-line-of-sight (NLoS) are two states of A2G channels, and each state has a distinct model. The work in [9] proposed a probabilistic LoS channel model to model the occurrence probability of LoS/NLoS state through the function with respect to UAV-ground elevation angle. Intuitively, the LoS probability increases with the UAV-ground elevation angle by increasing the altitude of the UAV or moving closer to user horizontally. If the UAV altitude increases, then the distances between the UAV and users increase, leading to larger path loss which reflects the angle-distance trade-off for altitude sensitive channel gain. When considering the UAV flight in the 3D communication networks, larger altitude of the UAV results in larger or approximately the same elevation angle

This work was supported by the National Natural Science Foundation of China under Grant 62172339. The corresponding author is Cheng Zhan.

between the UAV and all users, more fair communication and homogeneous delay may be achieved between the UAV and all users. However, increasing the UAV altitude leads to the increase of distance between the UAV and users as well, and the throughput of users reduces. In fact, the influence of UAV altitude on throughput and delay is uncertain, which has not been studied in prior work.

Motivated by the above, this paper aims to overcome the aforementioned limitations in the existing designs. In this paper, we focus on the fundamental tradeoff between throughput and delay over a 3D UAV communication network. By introducing minimum required rate for users to decipt delay requirement and guarantee fairness among users, our goal is to maximize the minimum weighted sum of throughput and required rate for all users. The elevation angle aware probabilistic LoS channel is adopted where angle-distance tradeoff is also unveiled for the 3D UAV communication network in this paper. The main contributions of this research can be itemized as follows:

- To characterize the fundamental tradeoff between throughput and delay over a 3D UAV communication network, we introduce the minimum required rate for users and aim to maximize the minimum weighted sum of throughput and required rate for each user, via joint optimization of the 3D UAV trajectory and communication time and rate allocation. The elevation angle aware probabilistic LoS channel and fairness among all users are also taken into account.
- The joint design problem is formulated as a non-convex optimization problem, where an iterative algorithm is proposed to obtain a suboptimal solution. Specifically, the problem is divided into two sub-problems, which are solved alternatively by using the block coordinate descent (BCD) method. The subproblems in each iteration are solved by employing successive convex approximation (SCA) and difference of two convex (D.C.) optimization methods.
- Extensive simulation results show that our proposed solution outperforms baseline schemes and unveils the interesting insights and tradeoff between throughput and delay as well as altitude related angle-distance tradeoff over 3D UAV communication networks.

II. System Model and Problem Formulation

In this paper, we consider a UAV communication system, where a UAV is employed as an ABS to provide services for K ground users (GUs), denoted by $\mathcal{S} = \{s_k | 1 \le k \le K\}$. The horizontal location of user s_k is denoted as $\mathbf{w}_k \in \mathbb{R}^{2\times 1}$. For ease of analysis, the time horizon T is divided into N equal-length time slots δ_t, i.e., $T = N\delta_t$. Thus, the horizontal location at time slot n of the UAV can be represented by $\mathbf{q}[n] \in \mathbb{R}^{2\times 1}$. We define $z[n]$ as the altitude of the UAV at time slot n, $H_{\min} \le z[n] \le H_{\max}$, where the allowable flight altitude of UAV ranges from $H_{\min}$ to $H_{\max}$. As a result, the UAV 3D location at time slot n is denoted as $(\mathbf{q}[n], z[n])$. We assume that $\mathbf{q}[1] = \mathbf{q}[N]$ and $z[1] = z[N]$ such that the UAV can serve GUs periodically. Due to the mechanical limitation of the UAV, we have $\|\mathbf{q}[n] - \mathbf{q}[n-1]\| \le \delta_t V_{xy}^{max}$, $|z[n] - z[n-1]| \le \delta_t V_z^{max}$, $2 \le n \le N$, where V_{xy}^{max} and V_z^{max} are the maximum speeds in horizontal and vertical directions, respectively. The distance between the UAV and user s_k at time slot n can be given by $d_k[n] = \sqrt{\|\mathbf{q}[n] - \mathbf{w}_k\|^2 + z[n]^2}$. The main notations in this paper are summarized in Table I.

TABLE I
Definition and Notation

Notation	Definition
K	The number of GUs
N	The number of time slots for time horizon T
δ_t	Elemental slot length (s)
H	The UAV altitude (m)
$\mathbf{w}_k$	The horizontal coordinate of GU s_k
$\mathbf{q}[n]$	UAV horizontal location at time slot n
$z[n]$	UAV altitude at time slot n
V_{xy}^{max}	The maximum speed in horizontal direction (m/s)
V_z^{max}	The maximum speed in vertical direction (m/s)
$\theta_k[n]$	The elevation angle between GU s_k and the UAV at time slot n
$R_k[n]$	The achievable rate between GU s_k and UAV at time slot n
$x_k[n]$	The fraction of time allocated at time slot n for communicating to GU s_k
D_k	The total throughput of GU s_k (bps)
r_k	The minimum required rate for s_k at each time slot (bps)
m	Weighting factor

A. Communication Model

In general, the A2G channels are characterized by the small-scale fading and large-scale channel coefficients, which depend on whether the A2G channels are LoS or NLoS channels. Although each time slot may contain multiple fading blocks, the effect can be averaged by using long channel codes [10]. Similar to [9], the LoS probability between the user s_k and UAV at time slot n, denoted by $\mathbb{P}_k^L[n]$, can be expressed as a logistic function with respect to the elevation angle $\theta_k[n]$, where $\theta_k[n] \triangleq \frac{180}{\pi} \arctan \frac{z[n]}{\|\mathbf{q}[n] - \mathbf{w}_k\|}$. Specifically,

$$\mathbb{P}_k^L[n] = B_c + \frac{B_d}{1 + e^{-(B_a + B_b \theta_k[n])}}, \tag{1}$$

where $B_a < 0, B_b > 0, B_d > 0,$ and $B_c = 1 - B_d,$ and all the constants depend on a certain environment. The large-scale channel power gain between the UAV and s_k at time slot n, denoted by $\beta_k[n]$, can be expressed as $\beta_k[n] = \beta_0 d_k[n]^{-\alpha_L}$ for LoS channel with probability $\mathbb{P}_k^L[n]$ and $\beta_k[n] = \rho\beta_0 d_k[n]^{-\alpha_N}$ for NLoS link with probability $1 - \mathbb{P}_k^L[n]$, where β_0 is the channel power gain at the reference distance 1 m, and the additional attenuation factor propagated by the NLoS link can be written as $\rho < 1$. In addition, the path loss exponents of LoS and NLoS channels can be expressed as α_L and α_N, respectively.

Denote $x_k[n]$ as the fraction of time allocated at time slot n for communicating with user s_k, $0 \le x_k[n] \le 1$. We assume that at most one GU can be scheduled for communication at each time instant, then we have $\sum_{k=1}^{K} x_k[n] \le 1, \forall n$. Let P denote the UAV's transmit power when a user is scheduled for communication. The achievable rate between the UAV and s_k can be written as $R_k[n] = B\log_2\left(1 + \frac{P\beta_k[n]}{\sigma^2}\right)$ in bits/second (bps), where B denotes the signal bandwidth

while σ^2 denotes the noise power. We assume that a sufficiently long channel code is adopted such that the effects of small-scale fading have been averaged in each time slot. Note that $R_k[n]$ depends on $\beta_k[n]$ which is closely related to the existence of LoS links. By following the probabilistic LoS model, we consider the expected rate $\mathbb{E}[R_k[n]]$, which can be approximated as in [10], i.e., $\mathbb{E}[R_k[n]] \approx B\Big(B_c + \frac{B_d}{1+e^{-(B_a+B_b\theta_k[n])}}\Big)\log_2\left(1+\frac{\gamma}{(\|\mathbf{q}[n]-\mathbf{w}_k\|^2+z_n^2)^{\alpha_L/2}}\right) \triangleq \bar{R}_k[n]$ with $\gamma \triangleq \frac{P\beta_0}{\sigma^2}$. In the following, we use $\bar{R}_k[n]$ for trajectory design as in [11]. As such, the overall throughput of GU s_k can be calculated as $D_k = \sum_{n=1}^{N} x_k[n]\bar{R}_k[n]$.

B. Problem Formulation

In the paper, we consider the delay-constrained services for users, e.g., video applications. A minimal required rate r_k is imposed for each user s_k, i.e., $x_k[n]\bar{R}_k[n] \geq r_k, \forall k, n$. For example, r_k may correspond to the playback rate required by user s_k for video streaming, and there exists no video stuck if the minimum playback rate is met. As such, $\frac{1}{r_k}$ represents for the delay requirement for user s_k at each time slot. Intuitively, more QoS provisioning can be obtained for each GU s_k with larger throughput and smaller delay. Therefore, we aim to maximize D_k and r_k simultaneously for each user s_k. To achieve the tradeoff between D_k and r_k, we simply associate each of them with a weighting coefficient and maximize the weighted sum, i.e., $mD_k + (1-m)r_kN$ with weighting factor m, $0 \leq m \leq 1$, where r_k is multiplied by N to make it comparable to the throughput. Let $\mathbf{Q} \triangleq \{\mathbf{q}[n]\}, \mathbf{X} \triangleq \{x_k[n]\}, \mathbf{Z} \triangleq \{z[n]\}, \mathbf{R} \triangleq \{r_k\}$. To enable fairness among all GUs, our aim is to maximize the minimum weighted sum among all GUs by optimizing the 3D UAV trajectory as well as communication time and rate allocation. Based on those models above, the optimization problem can be written by

$$
\begin{aligned}
(\text{P1}): \max_{\mu,\mathbf{Q},\mathbf{X},\mathbf{Z},\mathbf{R}} \ & \mu \\
\text{s.t.} \quad & 0 \leq x_k[n] \leq 1, \forall k, \forall n, && (2)\\
& \sum_{k=1}^{K} x_k[n] \leq 1, \forall n, && (3)\\
& mD_k + (1-m)r_kN \geq \mu, \forall k, && (4)\\
& x_k[n]\bar{R}_k[n] \geq r_k, \forall k, \forall n, && (5)\\
& \theta_k[n] = \frac{180}{\pi}\arctan\frac{z[n]}{\|\mathbf{q}[n]-\mathbf{w}_k\|}, \forall k, \forall n, && (6)\\
& H_{\min} \leq z[n] \leq H_{\max}, \forall n, && (7)\\
& \mathbf{q}[1] = \mathbf{q}[N], z[1] = z[N], && (8)\\
& |\, z[n] - z[n-1] \,| \leq \delta_t V_z^{max}, \forall n, && (9)\\
& \|\mathbf{q}[n] - \mathbf{q}[n-1]\| \leq \delta_t V_{xy}^{max}, \forall n. && (10)
\end{aligned}
$$

It can be verified that problem (P1) is a non-convex optimization problem due to the non-convex constraints in (4)-(6) with coupled variables and complicated expression of expected rate, which is difficult to solve directly.

III. Proposed Solution

In the following, we adopt the BCD method [12] to decouple the variables into multiple blocks and tackle the non-convex terms with D.C. optimization and SCA techniques. Specifically, with given UAV altitude, resource allocation and UAV 2D trajectory $\{\mathbf{Q}, \mathbf{X}, \mathbf{R}\}$ are optimized with D.C. optimization and SCA techniques. For any resource allocation and UAV 2D trajectory, we optimize the UAV altitude $\mathbf{Z}$ with SCA technique. The two subproblems are optimized alteratively until convergence.

A. Resource Allocation and 2D Trajectory Optimization

With given UAV altitude $\mathbf{Z}$, problem (P1) is reduced to

$$
\begin{aligned}
(\text{P2}): \max_{\mu,\mathbf{Q},\mathbf{X},\mathbf{R}} \ & \mu \\
\text{s.t.} \quad & (2)-(6), (10), \\
& \mathbf{q}[1] = \mathbf{q}[N]. && (11)
\end{aligned}
$$

By introducing slack variables $\mathbf{Y} \triangleq \{y_k[n]\}$, $\mathbf{\Theta} \triangleq \{\theta_k[n]\}$, we have the following problem,

$$
\begin{aligned}
(\text{P3}): \max_{\mu,\mathbf{Q},\mathbf{X},\mathbf{R},\mathbf{Y},\mathbf{\Theta}} \ & \mu \\
\text{s.t.} \quad & (2), (3), (10), (11), \\
& m\sum_{n=1}^{N} x_k[n]y_k[n] + (1-m)r_kN \geq \mu, \forall k, && (12)\\
& \bar{R}_k[n] \geq y_k[n], \forall k, \forall n, && (13)\\
& x_k[n]y_k[n] \geq r_k, \forall k, \forall n, && (14)\\
& \theta_k[n] \leq \frac{180}{\pi}\arctan\frac{z[n]}{\|\mathbf{q}[n]-\mathbf{w}_k\|}, \forall k, \forall n. && (15)
\end{aligned}
$$

It can be shown that in the optimal solution to (P3), the equalities hold in both (13) and (15). Otherwise, we can always increase $\theta_k[n]$ and $y_k[n]$ until the equalities hold, and other constraints are still met without changing the objective value. Thus, problem (P3) is equivalent to problem (P2). However, (P3) is still a non-convex optimization problem due to non-convex constraints in (12)-(15).

It is observed that the non-convex term $x_k[n]y_k[n]$ in (12) and (14) can be rewritten as a difference of convex functions, i.e., $x_k[n]y_k[n] = \frac{1}{2}(x_k[n]+y_k[n])^2 - \frac{1}{2}(x_k^2[n]+y_k^2[n])$, where D.C. optimization technique [13] can be adopted. Specifically, by applying first-order Taylor approximation on $\frac{1}{2}(x_k[n] + y_k[n])^2$ with given local point $x_k[n]^l$ and $y_k[n]^l$, we obtain

$$
\begin{aligned}
& x_k[n]y_k[n] \geq (x_k[n]^l + y_k[n]^l)(x_k[n] + y_k[n]) \\
& -\frac{1}{2}(x_k[n]^l + y_k[n]^l)^2 - \frac{1}{2}(x_k^2[n] + y_k^2[n]) \triangleq Q_k[n]^{lb}, && (16)
\end{aligned}
$$

where $Q_k[n]^{lb}$ is now joint concave with $x_k[n]$ and $y_k[n]$.

For (15), since $\arctan\frac{1}{x}$ is convex with $x > 0$, by applying first-order Taylor approximation over $\arctan$ function with given $\mathbf{q}[n]^l$, we have

$$
\begin{aligned}
& \arctan\frac{z[n]}{\|\mathbf{q}[n]-\mathbf{w}_k\|} \geq \arctan\frac{z[n]}{\|\mathbf{q}[n]^l-\mathbf{w}_k\|} \\
& +\Lambda_{k,n}(\|\mathbf{q}[n]-\mathbf{w}_k\| - \|\mathbf{q}[n]^l-\mathbf{w}_k\|) \triangleq v_k[n]^{lb}, && (17)
\end{aligned}
$$

where $\Lambda_{k,n} = \frac{-z[n]}{\|\mathbf{q}[n]^l-\mathbf{w}_k\|^2+z_n^2}$.

For (13), it can be verified that a function $\left(B_c + \frac{B_d}{x}\right)\log_2\left(1+\frac{\gamma}{(y)^{\alpha_L/2}}\right)$ is jointly convex with respect

to x and y. By applying first-order Taylor approximation over the above function with given $\mathbf{q}[n]^l$ and $\theta_k[n]^l$, we have

$$\bar{R}_k[n] \geq \Gamma_k[n]^l - \Omega_k[n]^l\Big(e^{-(B_a+B_b\theta_k[n])} - e^{-(B_a+B_b\theta_k[n]^l)}\Big) - \hat{\Psi}_k[n]^l(\|\mathbf{q}[n]-\mathbf{w}_k\|^2 - \|\mathbf{q}[n]^l-\mathbf{w}_k\|^2) \triangleq \bar{R}_k[n]^{lb}, \quad (18)$$

where $\Gamma_k[n]^l = B\left(B_c + \frac{B_d}{X_k[n]^l}\right)\log_2\left(1+\frac{\gamma}{(Y_k[n]^l)^{\alpha_L/2}}\right)$, with $X_k[n]^l \triangleq 1 + e^{-(B_a+B_b\theta_k[n]^l)}$ and $Y_k[n]^l \triangleq \|\mathbf{q}[n]^l-\mathbf{w}_k\|^2 + z[n]^2$, $\Omega_k[n]^l = \frac{BB_d(\log_2 e)}{(X_k[n]^l)^2}\ln\left(1+\frac{\gamma}{(Y_k[n]^l)^{(\alpha_L/2)}}\right)$, $\Psi_k[n]^l = B\left(B_c+\frac{B_d}{X_k[n]^l}\right)\frac{\gamma\alpha_L/2(\log_2 e)}{Y_k[n]^l\left((Y_k[n]^l)^{\frac{\alpha_L}{2}}+\gamma\right)}$.

By substituting the lower bounds derived in (16)-(18), (P3) is approximated as

$$\begin{aligned}(\text{P4}): \max_{\mu,\mathbf{Q},\mathbf{X},\mathbf{R},\mathbf{Y},\boldsymbol{\Theta}} \ & \mu \\ \text{s.t.} \ & (2),(3),(10),(11), \\ & m\sum_{n=1}^{N} Q_k[n]^{lb} + (1-m)r_kN \geq \mu, \forall k, \quad (19)\\ & \bar{R}_k[n]^{lb} \geq y_k[n], \forall k, \forall n, \quad (20)\\ & Q_k[n]^{lb} \geq r_k, \forall k, \forall n, \quad (21)\\ & \theta_k[n] \leq \frac{180}{\pi} v_k[n]^{lb}, \forall k, \forall n. \quad (22)\end{aligned}$$

It can be shown that (P4) is a standard convex optimization problem, which can be efficiently solved by solvers such as CVX [14]. With D.C. optimization and SCA techniques, the details of algorithm for solving problem (P2) can be given in Algorithm 1, whose complexity can be given by $O((NK)^{3.5}\log(1/\kappa))$ with solution accuracy κ.

Algorithm 1 Iterative algorithm for solving problem (P2)

1: Initialize $\{x_k[n]^0, y_k[n]^0, \mathbf{q}[n]^0, \theta_k[n]^0\}$, and let $l=0$;
2: **repeat**
3: With given local points $\{x_k[n]^l, y_k[n]^l, \mathbf{q}[n]^l, \theta_k[n]^l\}$, solve convex optimization problem (P4) with CVX to obtain optimal solution $\{x_k[n]^*, y_k[n]^*, \mathbf{q}[n]^*, \theta_k[n]^*\}$;
4: Update local points $x_k[n]^{l+1} = x_k[n]^*$, $y_k[n]^{l+1} = y_k[n]^*$, $\mathbf{q}[n]^{l+1} = \mathbf{q}[n]^*$, $\theta_k[n]^{l+1} = \theta_k[n]^*$;
5: Update $l = l+1$;
6: **until** Converge to a prescribed accuracy.

B. UAV Altitude Optimization

Given any feasible UAV 2D trajectory and resource allocation $\{\mathbf{Q},\mathbf{X},\mathbf{R}\}$, problem (P1) is reduce to

$$\begin{aligned}(\text{P5}): \max_{\mu,\mathbf{Z}} \ & \mu \\ \text{s.t.} \ & (4)-(7),(9), \\ & z[1] = z[N], \quad (23)\end{aligned}$$

which is equivalent to

$$\begin{aligned}(\text{P6}): \max_{\mu,\mathbf{Z},\boldsymbol{\Theta}} \ & \mu \\ \text{s.t.} \ & (4),(5),(7),(9),(15),(23),\end{aligned}$$

since we can always increase $\theta_k[n]$ until the equalities hold without changing the objective value. Note that $\bar{R}_k[n]$ is a non-concave function with respect to $z[n]$. Similar to (17), by using first-order Taylor approximation with given $\theta_k[n]^l$ and $z[n]^l$, we have

$$\bar{R}_k[n] \geq \tilde{\Gamma}_k[n]^l - \tilde{\Omega}_k[n]^l\left(e^{-(B_a+B_b\theta_k[n])} - e^{-(B_a+B_b\theta_k[n]^l)}\right) - \hat{\Psi}_k[n]^l(z[n]^2 - (z[n]^l)^2) \triangleq \tilde{R}_k[n]^{lb}, \quad (24)$$

where $\tilde{\Gamma}_k[n]^l = \left(B_c+\frac{B_d}{\tilde{X}_k[n]^l}\right)\log_2\left(1+\frac{\gamma}{(\tilde{Y}_k[n]^l)^{\alpha_L/2}}\right)$, with $\tilde{X}_k[n]^l \triangleq 1+e^{-(B_a+B_b\theta_k[n]^l)}$ and $\tilde{Y}_k[n]^l \triangleq \|\mathbf{q}[n]-\mathbf{w}_k\|^2 + (z[n]^l)^2$, $\tilde{\Omega}_k[n]^l = \frac{B_d(\log_2 e)}{(\tilde{X}_k[n]^l)^2}\ln\left(1+\frac{\gamma}{(\tilde{Y}_k[n]^l)^{(\alpha_L/2)}}\right)$, $\tilde{\Psi}_k[n]^l = \left(B_c+\frac{B_d}{\tilde{X}_k[n]^l}\right)\frac{\gamma\alpha_L/2(\log_2 e)}{\tilde{Y}_k[n]^l\left((\tilde{Y}_k[n]^l)^{\frac{\alpha_L}{2}}+\gamma\right)}$.

Based on (24), we can approximate (P6) with the following problem

$$\begin{aligned}(\text{P7}): \max_{\mu,\mathbf{Z},\boldsymbol{\Theta}} \ & \mu \\ \text{s.t.} \ & m\sum_{n=1}^{N} x_k[n]\tilde{R}_k[n]^{lb} + (1-m)r_kN \geq \mu, \forall k, \quad (25)\\ & x_k[n]\tilde{R}_k[n]^{lb} \geq r_k, \forall k, \forall n, \quad (26)\\ & (7),(9),(15),(23).\end{aligned}$$

It can be shown that problem (P7) is now a convex formulation which can be easily solved by CVX. Thus, the iterative algorithm for (P5) is similar to Algorithm 1 by applying the SCA technique with given $\theta_k[n]^l$ and $z[n]^l$ and solving convex optimization problem (P7) iteratively.

The overall algorithm for solving problem (P1) is summarized in Algorithm 2. The target value is non-decreasing in the iterative solution of subproblems (P2) and (P5), and then Algorithm 2 converges to a suboptimal solution [12]. In addition, the complexity of Algorithm 2 can be obtained by $O((NK)^{3.5}\log^2(1/\kappa))$.

Algorithm 2 Overall algorithm for solving problem (P1)

1: Initialize $\{x_k[n]^0, \mathbf{q}[n]^0, z[n]^0\}$, and let $r=0$;
2: **repeat**
3: With given $\{x_k[n]^r, \mathbf{q}[n]^r, z[n]^r\}$, solve problem (P2) with Algorithm 1 to obtain solution $\{x_k[n]^{r+1}, \mathbf{q}[n]^{r+1}\}$;
4: With given $\{x_k[n]^{r+1}, \mathbf{q}[n]^{r+1}, z[n]^r\}$, solve problem (P5) with similar Algorithm 1 to obtain solution $\{z[n]^{r+1}\}$;
5: Update $r = r+1$;
6: **until** Converge to a prescribed accuracy.

IV. Simulation Results

In this section, extensive simulations are conducted to evaluate the effectiveness of the proposed design. We assume that $K=5$ GUs are randomly distributed in a 800 m $\times$ 800 m square, where the parameters of the generalized logistic model can be set as $B_a = -0.4568$, $B_b = 0.0470$, $B_c = -0.63$,

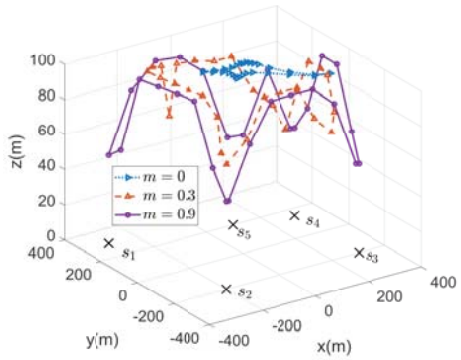

(a) 3D UAV trajectory versus m.

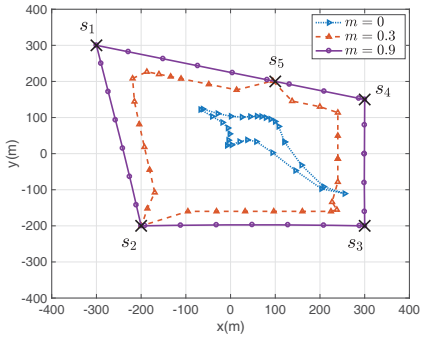

(b) 2D UAV trajectory versus m.

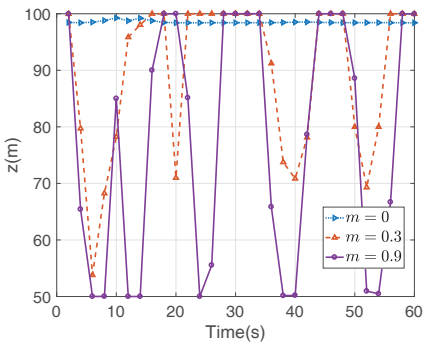

(c) UAV altitude versus m.

Fig. 1. The optimized UAV trajectory with different weighting factor m.

$B_d = 1.63$ as in [10]. The UAV's flying altitude ranges from $H_{\min} = 50$m to $H_{\max} = 100$m. The maximum horizontal and vertical flight speeds of UAV are set as $V_{xy}^{max} = 40$ m/s and $V_z^{max} = 20$ m/s, respectively. The initial UAV trajectory is set to be a circular trajectory centered at the centroid of all GUs over the altitude of $H_{\max}$. Similar to [12], the communication parameters are set as $P = 0.1$ W, $\beta_0 = -60$ dB, $B = 1$ MHz, $\sigma^2 = -110$ dBm, $\delta_t = 1$ s, $\alpha_L = 2.5$.

Fig. 1 shows the optimized UAV trajectory with different weighting factor m when $T = 60$ s. Fig. 1(a) describes the 3D UAV trajectory, while Fig. 1(b) and Fig. 1(c) show 2D UAV trajectory and UAV altitude, respectively. From Fig. 1, we can see that the optimized UAV trajectory varies with different values of m, where interesting insights can be obtained. With a large value of m, maximizing the throughput for each GU is more important, and the UAV is expected to move closer to each GU such that better channel quality can be achieved. In addition, the UAV altitude reduces when moving close to GU, where the distance between the UAV and GU can be further reduced to improve the communicating efficiency, as shown in 1(c). It is interesting to see that the UAV flies up and down frequently and tends to stay at high altitude until it approaches to GU. The reason is that the LoS probability between the UAV and GU depends on the elevation angle, where higher LoS probability can be achieved with higher altitude. The dominant factors impacting the channel quality differ in different periods. When the UAV approaches to GU, the impact of decreasing the distance is more influential, and then the UAV altitude reduces. However, when the UAV leaves that GU, the impact of elevation angle on channel quality is more significant and then the UAV's altitude increases. Another reason for the increasing of altitude is the fairness of data transmission among GUs, since the UAV may increase its altitude to rise the elevation for other GUs.

On the other hand, when m is small, maximizing the minimum required rate for each GU is more important, and the 2D UAV trajectory shrinks and the UAV keeps at the high altitude, as shown in Fig. 1(b) and Fig. 1(c). In other words, the UAV tends to hover over all GUs to avoid moving away from any GU. The reason is that large required rate for each GU should be satisfied at each time slot with small m. If the UAV gets far from one particular GU, then the required rate for that GU may not be achieved. Fig. 2 shows the communication time allocation for multiple GUs with different values of m. When $m = 0.3$, maximizing the minimum required rate for each GU is more important, and all users are scheduled in each time slot to satisfy minimum required rate. When $m = 0.9$, the impact of maximizing throughput is greater, and the UAV prefers to communicate with the GU when it is close enough to the GU with better channel quality, so as to enhance the communication efficiency which leads to smaller minimum required rate for each GU. Unless otherwise stated, we set $m = 0.9$.

Fig.3 depicts the tradeoff between throughput and minimum required rate of user with different values of m. It is shown that throughput increases at the cost of reducing minimum required rate with large m, which is in accordance with Fig. 1. In the practical application, m can be chosen appropriately to balance the tradeoff between throughput and delay with specific requirements. In order to show the advantages of the proposed joint design, we compare the max-min weighted sum of proposed solution with that achieved by the following schemes: 1) *2D fixed benchmark*, where the UAV stays at the centroid of all GUs with altitude being optimized as in [15]; 2) *Altitude fixed benchmark*, where the UAV flies at $H_{\max}$ and the 2D UAV trajectory is optimized as in [12]; 3)*Equal allocation benchmark*, where the communication time is equally allocated for all GUs; 4) *Static benchmark*, where the UAV stays at the centroid of all GUs with altitude $H_{\max}$. Fig. 4 shows the max-min weighted sum of throughput and required rate with different time horizon T. It is observed that the weighted sum increases with time T, as expected. Compared

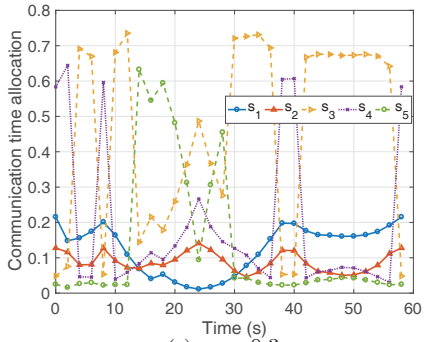

(a) $m = 0.3$.

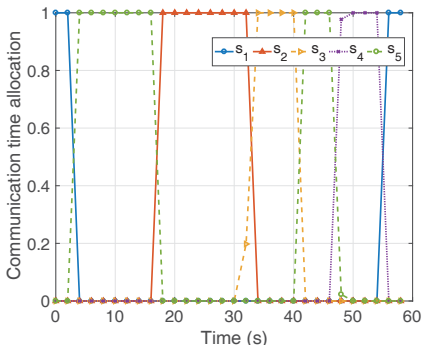

(b) $m = 0.9$.

Fig. 2. Communication time allocation among different GUs.

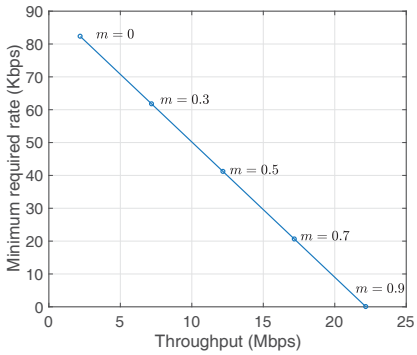

Fig. 3. Tradeoff between throughput and minimum required rate.

with other benchmarks, the proposed solution achieves the maximum weighted sum and is most conducive to the data communication between UAV and GUs. The performance gap between our proposed solution and equal allocation benchmark demonstrates the gain brought by communication time allocation. Compared with 2D fixed benchmark and altitude fixed benchmark as well as static benchmark, the additional gain brought by flexible 3D UAV mobility is demonstrated, which increases the effectiveness of information transmission.

V. Conclusion

A fundamental tradeoff between the throughput and delay over 3D UAV communication networks is studied in this paper. We introduce the minimum required rate for each GU and aim to maximized the minimum weighted sum of throughput and required rate for each user, via joint optimization of the 3D UAV trajectory and communication time and rate allocation.

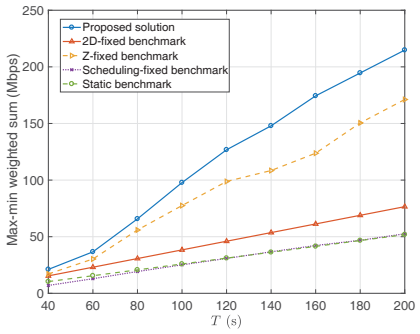

Fig. 4. The max-min weighted sum versus T.

The joint design is formulated as a non-convex optimization problem. We propose an iterative algorithm to achieve a suboptimal solution based on block coordinate descent and D.C. optimization as well as SCA techniques. Simulation results illustrate the pronounced gains of proposed solution and unveils the interesting insights and tradeoff between throughput and delay over 3D UAV communication networks.

References

[1] M. Mozaffari, A. T. Z. Kasgari, W. Saad, M. Bennis, and M. Debbah, "Beyond 5G with UAVs: foundations of a 3D wireless cellular network," *IEEE Trans. Wireless Commun.*, vol. 18, no. 1, pp. 357-372, Jan. 2019.

[2] Y. Zeng, Q. Wu, and R. Zhang, "Accessing from the sky: a tutorial on UAV communications for 5G and beyond," *Proc. IEEE.*, vol. 107, no. 12, pp. 2327-2375, Dec. 2019.

[3] L. Gupta, R. Jain, and G. Vaszkun, "Survey of important issues in UAV communication networks," *IEEE Commun. Surv. Tuts.*, vol. 18, no. 2, pp. 1123-1152, 2nd Quart. 2016.

[4] J. Lyu, Y. Zeng, and R. Zhang, "UAV-aided offloading for cellular hotspot," *IEEE Trans. Wireless Commun.*, vol. 17, no. 6, pp. 3988-4001, Jun. 2018.

[5] Q. Wu, G. Y. Li, W. Chen, D. W. K. Ng, and R. Schober, "An overview of sustainable green 5G networks," *IEEE Wireless Commun.*, vol. 24, no. 4, pp. 72-80, Aug. 2017.

[6] J. Lyu, Y. Zeng, and R. Zhang, "Cyclical multiple access in UAV-aided communications: a throughput-delay tradeoff," *IEEE Wireless Commun. Lett.*, vol. 5, no. 6, pp. 600-603, Dec. 2016

[7] Q. Wu and R. Zhang, "Common throughput maximization in UAV-enabled OFDMA systems with delay consideration," *IEEE Trans. Commun.*, vol. 66, no. 12, pp. 6614-6627, Dec. 2018.

[8] J. -H. Lee, K. -H. Park, Y. -C. Ko, and M. -S. Alouini, "Throughput maximization of mixed FSO/RF UAV-aided mobile relaying with a buffer," *IEEE Trans. Wireless Commun.*, vol. 20, no. 1, pp. 683-694, Jan. 2021.

[9] A. Al-Hourani, S. Kandeepan, and S. Lardner, "Optimal LAP altitude for maximum coverage," *IEEE Wireless Commun. Lett.*, vol. 3, no. 6, pp. 569-572, Dec. 2014.

[10] C. You and R. Zhang, "Hybrid offline-online design for UAV-enabled data harvesting in probabilistic LoS channels," *IEEE Trans. Wireless Commun.*, vol. 19, no. 6, pp. 3753-3768, Jun. 2020.

[11] C. Zhan and Y. Zeng, "Energy-efficient data uploading for cellular-connected UAV systems," *IEEE Trans. Wireless Commun.*, vol. 19, no. 11, pp. 7279-7292, Nov. 2020.

[12] Y. Zeng and R. Zhang, "Energy-efficient UAV communication with trajectory optimization," *IEEE Trans. Wireless Commun.*, vol. 16, no. 6, pp. 3747-3760, Jun. 2017.

[13] B. Soleimani, and M. Sabbaghian, "Cluster-based resource allocation and user association in mmWave femtocell networks," *IEEE Trans. Commun.*, vol. 68, no. 3, pp. 1746-1759, Mar. 2020.

[14] M. Grant and S. Boyd. CVX: MATLAB Software for Disciplined Convex Programming, Version 2.1. Accessed: Dec. 9, 2018. [Online]. Available: http://cvxr.com/cvx

[15] Y. Chen, H. Zhang, and Y. Hu, "Optimal power and bandwidth allocation for multiuser video streaming in UAV relay networks," *IEEE Trans. Veh. Techn.*, vol. 69, no. 6, pp. 6644-6655, Jun. 2020.